IUBMB *Life*, 54: 241–252, 2002

1521-6543/02 $12.00 + .00
DOI: 10.1080/15216540290114540

Review Article

The Energetics of Ion Distribution: The Origin of the Resting Electric Potential of Cells

Richard L. Veech, Yoshihiro Kashiwaya, Denise N. Gates, M. Todd King, and Kieran Clarke[1]

LMBB/NIAAA, 12501 Washington Ave, Rockville, Maryland 20852, USA
[1]Department of Biochemistry, University of Oxford, South Parks Rd, Oxford, OX1 3QU, United Kingdom

Summary

The relation between the energies of ion movement and ATP hydrolysis is unknown in tissues with widely varying electric potentials. Consequently, we measured the concentration of the nine major inorganic ions in the extra- and intracellular phases in heart, liver, and red cells with resting electrical potentials, E_N, of −86, −28, and −6 mV, respectively, under six different physiological conditions. We calculated the Nernst electric potential and the energy of ion movement between the phases. We found that the energy of ATP hydrolysis was essentially constant, between −54 and −58 kJ/mol, in all tissues and conditions. In contrast, as E_N decreased, the energies of the Na^+ and K^+ gradients decreased, with slopes approximating their valence. The difference between the energies of Na^+ and K^+ gradients remained constant at 17 kJ/mol, which is approximately one third of the energy of ATP hydrolysis, demonstrating near-equilibrium of the Na^+/K^+ ATPase in all tissues under all conditions. All cations, except K^+, were pumped out of cells and all anions, except Cl^- in liver and red cell, were pumped into cells. We conclude that the energy of ATP was expressed in Na^+/K^+ ATPase and its linked inorganic ion transporters to create a Gibbs-Donnan near-equilibrium system, an inherent part of which was the electric potential.

IUBMB *Life*, 54: 241–252, 2002

Keywords ΔG′ of ATP hydrolysis; Gibbs-Donnan equilibrium; ion gradients; membrane potential.

INTRODUCTION

The electric potential resulting from the distribution of an ion between two phases, for example, the extra- and intracellular phases of cells, $E[ion^z]_{o/i}$, but not the energy of its distribution, is given by the Nernst equation (*1*):

$$E[ion^z]_{o/i} = \frac{RT}{zF} \ln \frac{[ion^z]_o}{[ion^z]_i} \quad [1]$$

where R is the gas constant of 8.31×10^{-3} kJ/mol/K, T is body temperature of 311.15 K, z is the valence of the ion, and F is the Faraday constant of 9.65×10^4 C/mol or 96.49 kJ/mol/V. If an ion is free to move between phases, such as via an open ion channel, a Nernst electric potential, E_N, is created.

The energy cost of moving an ion of valence $z^{\pm}$ from the intra- to the extracellular phase, $\Delta G'[ion^z]_{o/i}$, is:

$$\Delta G'[ion^z]_{o/i} = RT \ln \frac{[ion^z]_o}{[ion^z]_i} - zE_N F \quad [2]$$

The first term on the right side of Eq. [2] defines the concentration work and the second term defines the electrical work required to move a charged ion between phases of different electrical potential, E_N. In a Gibbs-Donnan equilibrium system (*2*, *3*), formed when an impermeant charged material is present on one side of a water-permeant rigid membrane, the ratios of all the permeant ion concentrations conform to the Nernst potential defined in Eq. [1]. In addition to the concentration and electrical work terms (Eq. [2]), the Gibbs-Donnan system includes a pressure work term, required to equalize the activity of water in both phases, and is given by the Van't Hoff equation (*4*):

$$\Pi V = nRT \quad [3]$$

where Π is osmotic pressure in atmospheres, V is volume in litres, n is the amount of a substance in moles, R is 82.06×10^{-3} litre-atmospheres/mol/K, and 1 kJ is 9.87 litre-atmospheres. Therefore, three types of work have been done on the system—electrical work, concentration work, and pressure work—the sum of which must be zero. High intracellular concentrations

Received 26 August 2002; accepted 9 October 2002.
Address correspondence to Richard L. Veech, LMBB/NIAAA, 12501 Washington Ave., Rockville, Maryland 20852. Fax: 301-443-0930; E-mail: rveech@mail.nih.gov

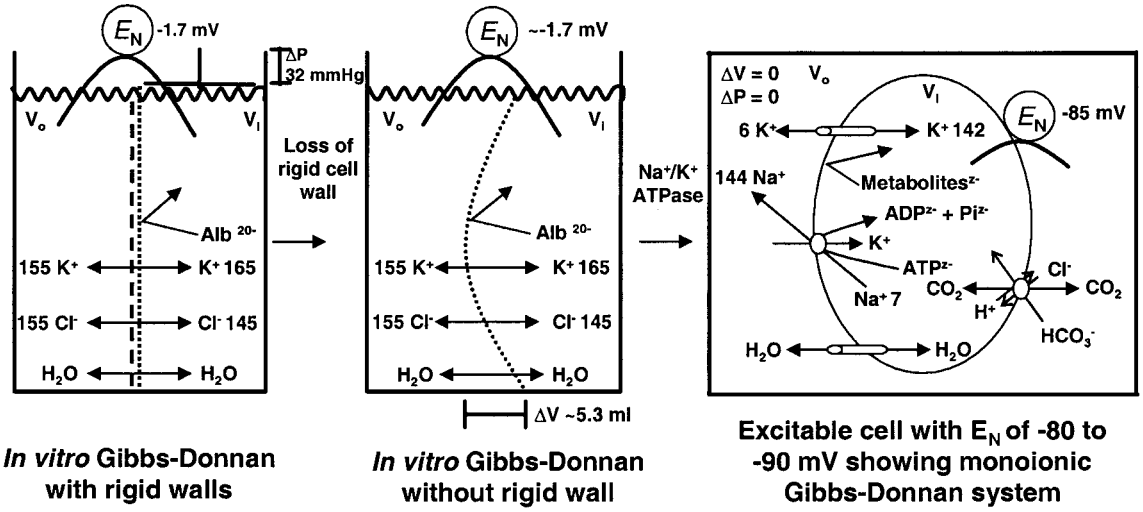

Figure 1. The Gibbs-Donnan equilibrium in inert systems and in an animal cell. If 1 mM of albumin containing 20 charges per mole is added to one side of a solution of 150 mM KCl solution separated by a membrane permeant to small ions, and the system not allowed to expand in volume, the equilibrium state is depicted in the left-hand panel. The electrical potential developed would be −1.7 mV and the pressure would be 32 mmHg. [For the method of calculation see *44*.] The side containing albumin would have an increased K^+ concentration and a decreased Cl^- concentration, whereas the activity of H_2O would be the same in both compartments. The system has performed electrical, concentration, and pressure work in coming to equilibrium where the sum of these energies is now 0. If the ion permeant membrane were allowed to expand, so that the pressure term became 0, the side containing the albumin would gain about 5.3 ml of H_2O (center panel). Animal cells, unlike plant or bacterial cells, lack a rigid cell wall and overcame the pressure dilemma by developing the Na pump, which created a functionally impermeant gradient of all cations in the extracellular space and, at the same time, increased the anionic concentration in the intracellular space, thus increasing the electric potential between the phases, but leaving the pressure and volume terms at zero (right panel).

of impermeant polyanions, such as ATP^{4-} and PCr^{2-}, form Donnan active materials, which would cause cells with nonrigid walls to swell (Fig. 1) because lipoprotein membranes are unable to bear pressure. To maintain volume, the Na^+/K^+ ATPase evolved to create functionally impermeant cations in the extracellular phase (*5*, *6*), thus equalizing the activity of free water in both phases. The distribution of any ion with a Nernst potential that does not equal E_N, constitutes charged, functionally impermeant Gibbs-Donnan active material.

It has been known for many years that the generation of ionic gradients characteristic of living cells requires metabolic energy (*7*). In the 1960s, the enzymatic basis for the creation of the high extracellular Na^+ and high intracellular K^+ by the Na pump (EC 3.6.1.37) was established (*8*). Much later it was recognized that the energy of ATP hydrolysis, $\Delta G'_{ATP}$, was fully expressed in the Ca^{2+} (*9*) and Na^+ concentration gradients, $\Delta G'[Na^+]_{o/i}$ (*10*). In turn, the $\Delta G'[Na^+]_{o/i}$ was linked to the energy of the other major inorganic ion gradients and to E_N. The formalism relating $\Delta G'_{ATP}$ in heart to the ionic movements catalysed by the electrogenic Na pump (EC 3.6.1.37),

$$3Na_i^+ + 2K_o^+ + ATP \leftrightarrow 3Na_o^+ + 2K_i^+ + ADP + Pi$$

combined with an open K^+ channel,

$$K_o^+ \leftrightarrow K_i^+$$

was the electroneutral, osmoneutral statement:

$$\Delta G'^{o}_{ATP\ Hydrolysis} - RT \ln \frac{[\Sigma ATP]}{[\Sigma ADP][\Sigma Pi]} + RT \ln \frac{[Na^+]_o^3[K^+]_i^3}{[Na^+]_i^3[K^+]_o^3} = 0 \quad [4]$$

In heart, the $\Delta G'[K^+]_{o/i}$ was 0, the $\Delta G'[Na^+]_{o/i}$ was one third of the $\Delta G'_{ATP}$, and the energies of the other inorganic ion gradients were derived from, and linked to, $\Delta G'[Na^+]_{o/i}$.

In tissues without open K^+ channels, in which Cl^- is the most permeant ion, no obvious set of ion movements have been assigned that result in the electroneutral, osmoneutral stoichiometry required for a steady state of constant volume and electric potential between phases. The object of this study was to determine whether the establishment of inorganic ion gradients is determined by $\Delta G'_{ATP}$ in heart under different conditions and in low-voltage tissues without open K^+ channels. We therefore measured the intracellular metabolites required to calculate the $\Delta G'_{ATP}$ and the gradients of the major inorganic ions across the plasma membrane in isolated, working rat heart perfused with glucose, with or without insulin or ketone bodies, in liver under normal conditions and during the metabolism of acetate, which causes large perturbations in inorganic ion transport by increasing the influx of Ca^{2+}, Mg^{2+}, and Pi (*11*), and in red cells. We

determined the $\Delta G'_{ATP}$, the Nernst potential of each inorganic ion, $E[ion^z]_{o/i}$, and the energy of each inorganic ion gradient between phases, $\Delta G'[ion^z]_{o/i}$, in the three tissues with a wide E_N range to determine what relations, if any, existed among these parameters.

METHODS AND MATERIALS

Animals. Ad lib fed male Wistar rats (Charles River) weighing between 300 and 450 g were used for all experiments. The NIAAA/NIH Animal Care and Use Committee, the University of Oxford Ethics Committees, and the Home Office (London) approved the experimental protocols.

Tissues. Working rat hearts ($n = 18$) were prepared as previously described (*10*) and perfused with modified Krebs-Henseleit buffer containing 10 mM glucose ($n = 8$), to which was added 100 nM insulin ($n = 5$) or 4 mM D-β-hydroxybutyrate and 1 mM acetoacetate ($n = 5$) (*12*). Freeze-clamped rat liver tissue was obtained 30 min after intraperitoneal administration of normal saline ($n = 11$) or Na acetate ($n = 6$) sufficient to achieve peak blood concentrations of 20 mM acetate (*11*). Erythrocytes were obtained by drawing blood from nonanaesthetized rats ($n = 7$) via a heparinized cannula implanted in the vena cava as previously described (*13*).

Calculations of Intracellular Ion Content. After determining metabolite content in μmol/g wet weight tissue, the data were converted to μmol/ml total tissue water from the total water content of the tissue. Intracellular tissue ion concentrations were determined using the equation:

$$[Ion]_{\mu mol/ml\ total\ water} - [Ion]_{EC} \times \%H_2O_{EC} = [Ion]_{IC} \times \%H_2O_{IC} \quad [5]$$

where $\%H_2O_{EC} + \%H_2O_{IC}$ are expressed as fractions with a sum of 1.

Tissue Water Distribution and Vascular Space. Tissue water distribution was determined by injection of ^3H_2O and ^{14}C-carboxyinulin (*13*). Hepatic vascular space was determined by incubating erythrocytes with $Na_2{}^{51}CrO_4$ and infusing the labeled cells into the jugular vein followed by a saline flush. Twenty minutes after infusion, an aliquot of blood was taken from the cannula for counting. Following cervical dislocation, a portion of liver was removed for counting. Hepatic vascular space was determined by comparing the total hepatic counts versus the activity observed in the whole blood sample.

Speciation of Extracellular Fluid Components. Total extracellular ion composition was measured in plasma for liver and erythrocyte experiments. For heart experiments, a Krebs-Henseleit bicarbonate medium was used as previously reported (*10*). After entering measured data for total magnesium, calcium, bicarbonate, phosphate, sodium, and potassium, along with hydrogen ion concentration and an estimated protein concentration, the ions were speciated as previously described (*10*) by solving a set of simultaneous equations using SEQS (CET Research Group, Ltd., Norman, OK) or Mathematica (Wolfram Research, Champaign, IL) software applications. Acid dissociation and stability constants at I = 0.15 or 0.25 and 38 °C for most metabolite species were from Kwack and Veech (*14*), Masuda et al. (*10*), Veech et al. (*15*), Walser (*16*), and Veloso et al. (*17*). Constants for carbonates and related species were taken from Sillen and Martell (*18*).

Inorganic Ion Measurements. For analysis of total tissue content of Na^+, Mg^{2+}, Ca^{2+}, and K^+, a sample of tissue (~50 mg) was digested overnight at 80 °C in 1 ml of concentrated nitric acid. After diluting in deionized water, the samples were analyzed on a Perkin-Elmer Model 3030 Atomic Absorption Spectrophotometer. Tissue concentrations were determined from standard curves of each metal run concurrently with the samples. Free magnesium was calculated from the measured ratio of [citrate]/[isocitrate] (*17*). Free magnesium in plasma and erythrocytes was taken to be 0.5 mM (*19*). Intracellular free calcium was taken to be 0.2 μM in all tissues (*9*).

For Cl^- determination tissue samples were extracted in 0.083 M sulfuric acid and neutralized with sodium tungstate, after the method of Funder and Wieth (*20*), and analyzed using a Corning Model 925 Chloride Analyzer. Whole tissue bicarbonate was determined enzymatically (*21*). Tissue pH was determined using ^{31}P magnetic resonance spectroscopy in heart (*22*, *23*) or from the measured venous $[CO_2]$/tissue $[HCO_3^-]$ in liver and red cell (*24*) and applying the Henderson-Hasselbalch equation (*25*). Heart free phosphate species were calculated (*23*) from free cytosolic [ΣPi] determined using magnetic resonance spectroscopy and corrected for intracellular pH and free $[Mg^{2+}]$ (*22*, *12*). Because obtaining free cytosolic Pi in liver required anesthesia with attendant changes in hepatic circulation, an alternative method for determining free cytosolic [ΣPi] was used. This method took advantage of the near-equilibrium of the purine-nucleoside phosphorylase (EC 2.4.2.1) and phosphopentomutase (EC 5.4.2.7) reactions in liver (*26*). Measurement of liver guanine, guanosine, and ribose-5-P contents allowed estimation of the free cytosolic [ΣPi] from the relationship:

$$[\Sigma Pi] = \frac{[Guanine][ribose\text{-}5\text{-}P]}{[Guanosine] \times K_{PNP} \times K_{PGM}} \quad [6]$$

where $K_{PNP} = 108$ and $K_{PGM} = 26$ at I = 0.25, pH 7.0, free $[Mg^{2+}] = 1$ mM and temperature = 38 °C (*26*).

Guanine and guanosine were measured by HPLC using a C18 column and phosphate gradient, and ribose-5-P was measured enzymatically (*27*). The mono- and divalent species of phosphate were estimated by solving the set of equations above, where binding (1/78.3) and acid dissociation (1.96×10^{-7}) constants had been adjusted to $I = 0.25$ and the free magnesium and hydrogen concentrations used were those prevailing in intracellular conditions.

Tissue and Ion Voltage Determinations. The E_N of heart was taken from the measured Nernst potential of K^+ distribution (Eq. [1]), which agreed well with KCl microelectrode

measurements (*28*). Those for liver and red cell were assigned from the measured Cl^- distribution as calculated from the Nernst equation (Eq. [1]), shown in liver to agree well with intracellular KCl microelectrode measurements (*15*).

Calculations of $\Delta G'[ion^z]_{o/i}$ *and* $\Delta G'_{ATP}$. The energy of ion distribution between the extra- and intracellular phase, $\Delta G'[ion^z]_{o/i}$, was calculated using the measured concentrations of the ions in the extra- and intracellular phases and the electric potential between the phases (Eq. [2]).

The $\Delta G'$ of ATP hydrolysis, $\Delta G'_{ATP}$, for each tissue was calculated as described previously (*10, 12, 29*) from the $\Delta G^{o'}$ of ATP hydrolysis determined at 38 °C, ionic strength of 0.25, and specified free $[Mg^{2+}]$ and pH (*30*). The $\Delta G'$ of ATP hydrolysis was then calculated for the sum species of products over reactants of the ATP hydrolysis reaction:

$$\Delta G'_{\text{ATP Hydrolysis}} = \Delta G^{o'}_{\text{ATP Hydrolysis}} + RT \ln \frac{[\Sigma\text{ADP}][\Sigma\text{Pi}]}{[\Sigma\text{ATP}]} \quad [7]$$

where [ΣATP], [ΣADP], and [ΣPi] indicates all ionic species present in the tissue.

The ratio of [ΣADP][ΣPi]/[ΣATP] in tissue was determined in red cell and liver from the measured reactants of the combined glyceraldehyde 3-P dehydrogenase (EC 1.2.1.12), 3 phosphoglycerate kinase (EC 2.7.2.3), triosphosphate isomerase (EC 5.3.1.1), and lactate dehydrogenase (EC 1.1.1.27) reactions (*29*) whereas the ratio in heart was determined from the measured concentrations of the reactants of creatine kinase reaction (EC 2.7.3.2) as described previously (*10, 12, 23, 29*).

RESULTS

Water Distribution. The water distribution of working perfused hearts was previously determined to be 59.3% extracellular and 40.7% intracellular (*10*). In freeze-clamped liver, the total water was 0.70 ml/g wet weight in controls and 0.65 ml/g wet weight in acetate treated rats. Extracellular H_2O was 26.6% in control and 28.3% in acetate-treated rat liver, whereas intracellular H_2O was 71.2% and 69.8% in the respective groups, with red cell water making up the difference. Whole blood contained 0.846 g of H_2O per ml and plasma 0.938 g/ml, with average hematocrit being 0.411. In whole blood, the red cell water was 31.4% and the extracellular water was 68.6%.

Metabolite Changes. Intracellular [Glucose] and [Glu-6-P] were elevated by administration of insulin to perfused hearts or Na acetate to liver (Table 1). Addition of insulin increased dihydroxyacetone-P [DHAP] in heart, whereas pyruvate [pyr] was decreased in heart by addition of both ketone bodies and insulin. Intracellular [citrate] and [isocitrate] were increased by insulin or ketone bodies in heart and by Na acetate in liver. Heart $[CO_2]$ was decreased during addition of ketone bodies. Heart $[NH_4^+]$ and L-glutamate [Glut] were increased by insulin or ketone bodies.

The free $[Mg^{2+}]$ decreased in perfused hearts treated with insulin or ketone bodies (Table 2) and increased in livers treated

Table 1
Metabolite contents in perfused heart, liver, and red cell

	Heart		Liver			Red cell
	Glucose (8)	G + Insulin (5)	G + Ketones (5)	Control (11)	Acetate (6)	Whole blood (7)
[Glucose]	5.72 ± 0.17	9.05 ± 0.38*	6.24 ± 0.39	6.75 ± 0.25	12.5 ± 0.7*	
[Glu-6P]	0.0586 ± 0.004	0.440 ± 0.007*	0.212 ± 0.028*	0.117 ± 0.009	0.428 ± 0.073*	
[DHAP]	0.0124 ± 0.002	0.0191 ± 0.0003*	0.0060 ± 0.0014	0.0226 ± 0.0015	0.0263 ± 0.0018	0.0170 ± 0.0010
[3PG]	0.0248 ± 0.0015	0.0223 ± 0.0061	0.0219 ± 0.0012	0.256 ± 0.015	0.346 ± 0.040	0.073 ± 0.004
[PEP]	0.0045 ± 0.0011	0.0038 ± 0.0022	0.0030 ± 0.0030		0.200 ± 0.008	
[Pyr]	0.0139 ± 0.0012	0.0079 ± 0.0010*	0.0079 ± 0.0007*	0.0699 ± 0.0087	0.0835 ± 0.0177	0.068 ± 0.008
[Lact]	0.237 ± 0.018	0.256 ± 0.027	0.100 ± 0.022*	0.491 ± 0.075	0.676 ± 0.076*	0.921 ± 0.231
[Citrate]	0.151 ± 0.015	0.307 ± 0.011*	0.400 ± 0.026*	0.366 ± 0.021	1.24 ± 0.04*	
[Isocitrate]	0.0066 ± 0.0005	0.0175 ± 0.0008*	0.0227 ± 0.0013*	0.0247 ± 0.0017	0.0579 ± 0.0033*	
$[CO_2]$	1.33 ± 0.02	1.31 ± 0.04	1.13 ± 0.01*	1.40 ± 0.04	1.38 ± 0.09	
[αKG]	0.0160 ± 0.0018	0.0159 ± 0.0030	0.0182 ± 0.0016	0.226 ± 0.013	0.210 ± 0.033	
$[NH_4^+]$	0.324 ± 0.009	0.486 ± 0.027*	0.571 ± 0.007*	0.724 ± 0.046	0.720 ± 0.057	
[Glut]	0.809 ± 0.069	4.49 ± 0.14*	4.61 ± 0.18*	4.59 ± 0.20	4.56 ± 0.31	
[ATP]	3.19 ± 0.14	3.80 ± 0.16*	3.42 ± 0.20	2.88 ± 0.07	2.46 ± 0.04*	2.25 ± 0.13
[ADP]	1.08 ± 0.06	0.809 ± 0.051	0.748 ± 0.028	1.06 ± 0.12	1.19 ± 0.08	0.248 ± 0.009
[AMP]	0.183 ± 0.013	0.133 ± 0.011	0.123 ± 0.008	0.166 ± 0.012	0.425 ± 0.022*	0.022 ± 0.001
$[Pi]_{total}$	4.70 ± 0.31	3.47 ± 0.18	3.67 ± 0.24	3.12 ± 0.14	4.06 ± 0.42	1.66 ± 0.06

Values are means ± SEM in units of μmol/g wet weight. The number of animals is given in parentheses. The significance of the difference of means in heart and liver data was judged by the Wilcoxon test with $P < 0.05$ indicated by *.

Table 2
Free pyridine nucleotide ratios, pH, ΔG of ATP hydrolysis, and E_N calculated from measured metabolites or ions

	Heart		Liver			Red cell
	Glucose (8)	G + Insulin (5)	G + Ketones (5)	Control (11)	Acetate (6)	Whole blood (7)
pH	7.06 ± 0.00	7.05 ± 0.01	7.04 ± 0.01	7.13 ± 0.03	7.23 ± 0.04	7.2
Free $[Mg^{2+}]$, mM	1.23 ± 0.03	$0.723 \pm 0.031^*$	$0.743 \pm 0.108^*$	0.392 ± 0.054	0.970 ± 0.098	0.5
$[NAD^+/NADH]_c$	1642 ± 248	1185 ± 291	$670 \pm 84^*$	764 ± 69	$521 \pm 116^*$	
$[NAD^+/NADH]_m$	16.0 ± 1.0	$4.63 \pm 0.61^*$	$1.51 \pm 0.03^*$	5.32 ± 0.39	3.90 ± 0.61	
$[NADP^+/NADPH]_c$	0.0034 ± 0.0006	$0.0012 \pm 0.0002^*$	$0.00095 \pm 0.0001^*$	0.0115 ± 0.0011	$0.00451 \pm 0.00089^*$	
$(ATP/ADP^*Pi)_c$, M^{-1}	11300 ± 700	$28800 \pm 1700^*$	$17800 \pm 900^*$	6920 ± 1280	7770 ± 1850	5700 ± 540
ΔG_{ATP}, kJ/mol	-56.0 ± 0.2	$-58.9 \pm 0.1^*$	$-57.6 \pm 0.2^*$	-56.5 ± 0.4	-56.1 ± 0.8	-57.3 ± 0.4
E_K, mV	-85.2 ± 0.0	-86.3 ± 0.0	-85.1 ± 0.0			
E_{Cl}, mV				-27.5 ± 1.9	-33.4 ± 2.0	-5.95 ± 0.59

For method of calculation, see text. Values are given as means ± SEM, with the number of observations given in parentheses. The significance of the differences of the means was judged by the Wilcoxon test, with $P < 0.5$ indicated by*.

with Na acetate. The free cytosolic [NAD^+]/[NADH] decreased in hearts treated with ketones and the free mitochondrial [NAD^+]/[NADH] decreased in heart after either insulin or ketone treatment. The free cytosolic [$NADP^+$]/[NADPH] was decreased in perfused heart by insulin or ketones and in liver by treatment with Na acetate. The cytosolic [ΣATP]/[ΣADP][ΣPi] increased in perfused heart during addition of insulin or ketones as did the negativity of the $\Delta G'$ of ATP hydrolysis.

The Electric Potential of the Inorganic Ions Between Phases E*[ion]*$_{o/i}$. The electric potential of the cations: $E[Ca^{2+}]_{o/i}$, $E[Na^+]_{o/i}$, $E[Mg^{2+}]_{o/i}$, and $E[K^+]_{o/i}$, differed widely, but were essentially invariant over the range of E_N (Fig. 2). $E[Ca^{2+}]_{o/i}$ was 115 mV, $E[Na^+]_{o/i}$ ranged around 85 mV, $E[Mg^{2+}]_{o/i}$ was essentially 0 mV, and $E[K^+]_{o/i}$ ranged about −85 mV. The E_N of heart calculated from the measured [K^+] in extra- and intracellular phases (Eq. [2]) was −85 to −86 mV, agreeing well with previous intracellular KCl microelectrode readings of −83 mV (*28*). The E_N of liver, measured from the distribution of $[Cl^-]_{o/i}$, ranged from −27.5 in control liver to −33 mV in acetate treated liver, agreeing well with the KCl microelectrode measurement in control livers of −28 mV (*15*). The E_N of red cell, calculated from Cl^- distribution, was −6 mV, in agreement with previous estimates (*20*). No microelectrode studies of E_N in red cell are available.

In contrast to the constant $E[\text{cation}]_{o/i}$ with different E_N, the variations of $E[\text{anion}]_{o/i}$ with E_N were nonlinear and second order (Fig. 2). $E[HCO_3^-]_{o/i}$ differed only slightly from $E[H^+]_{o/i}$, as would be expected from the permeance of CO_2 across cell membranes. $E[H_2PO_4^-]_{o/i}$ showed the most marked variation, being 73 mV in ketone-perfused hearts, 70 mV in controls, and 61 mV in insulin-perfused hearts. In liver, $E[H_2PO_4^-]_{o/i}$ decreased to 8 mV in control liver and to −33 mV in acetate-treated liver, in which phosphate influx was markedly increased. In red cell, $E[H_2PO_4^-]_{o/i}$ was about −10 mV. The $E[HPO_4^{2-}]_{o/i}$ followed the same pattern as $E[H_2PO_4^-]_{o/i}$, but was lesser in magnitude in all tissues. The $E[Cl^-]_{o/i}$ was −26 ± 2 mV in control hearts, −40 ± 5 mV in insulin-treated hearts, and −37 ± 8 mV in hearts perfused with ketones. In control liver, $E[Cl^-]_{o/i}$ was −28 ± 2 mV and −30 ± 2 mV after acetate treatment. In red cell, $E[Cl^-]_{o/i}$ was −6.0 ± 0.6 mV. In heart, E_N measured by KCl microelectrodes (*28*) was the same as $E[K^+]_{o/i}$, whereas in liver, E_N measured by intracellular KCl electrodes (*15*) was

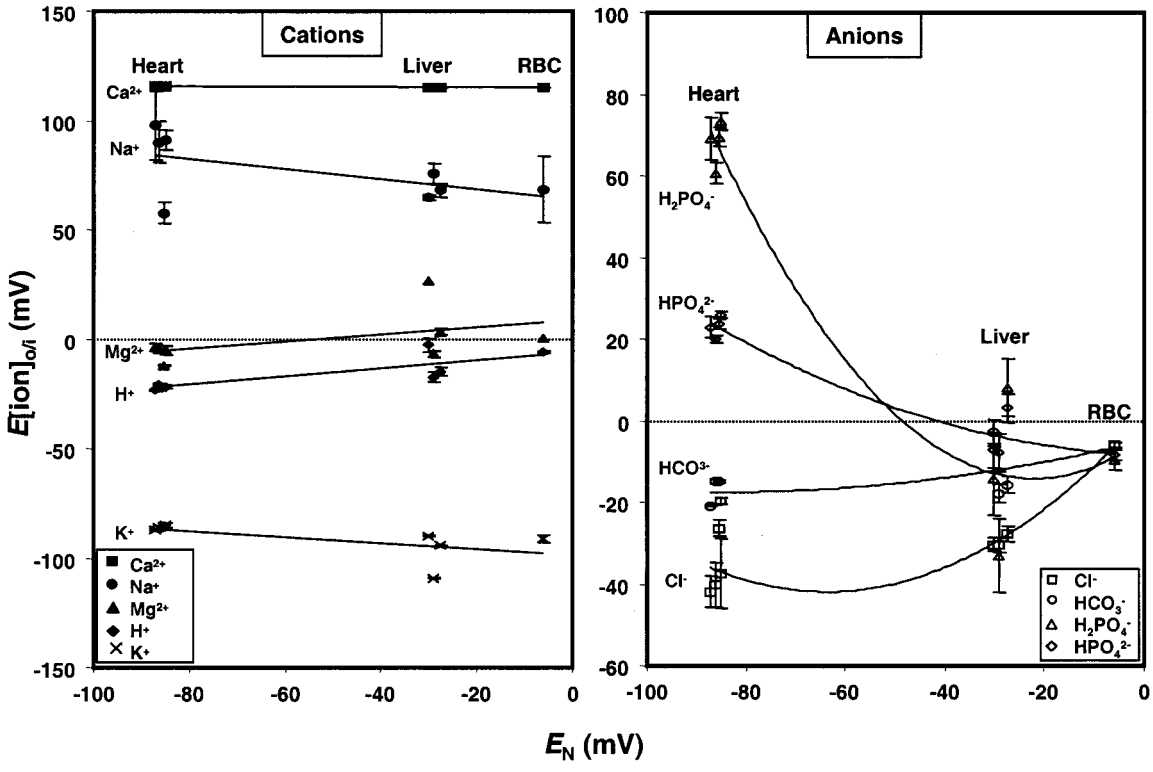

Figure 2. The Nernst potentials of the inorganic ions in tissues with differing measured electrical potentials, E_N, between intra- and extracellular phases. Th mean $E[\text{ion}^{\pm z}] \pm$ SEM (*n* given in Materials and Methods) were calculated from $E[\text{ion}^z]_{o/i} = \frac{RT}{zF} \ln \frac{[\text{ion}^z]_o}{[\text{ion}^z]_i}$ (Eq. [1]). $E[Ca^{2+}]_{o/i}$ and $E[Na^+]_{o/i}$ had large positive electric potentials of 115 and 68 to 90 mV, respectively, in all tissues. $E[K^+]_{o/i}$ was −85 to −86 mV in heart, reflecting the resting E_N measured by intracellular microelectrodes. Opening of Na channels in heart results in an action potential approaching that of $E[Na^+]_{o/i}$. $E[Cl^-]_{o/i}$ was −26 to −40 mV in heart, differing widely from $E[K^+]_{o/i}$. $E[Cl^-]_{o/i}$ was equal to E_N in liver and red cell, showing that Cl^- was the most permeant ion in these two tissues. Opening of a K^+ channel in lower voltage tissue, as a result of hormonal or other stimulation, would lead to hyperpolarization.

the same as $E[Cl^-]_{o/i}$. The $E[ion]_{o/i}$ of all anions intersected at -6 mV, suggesting that the negativity of red cell was due entirely to the impermeant metabolite polyanions with no contribution from permeant anions.

The Energy of Ion Gradients, $\Delta G'[ion^z]_{o/i}$, Between Extra- and Intracellular Phases. The $\Delta G'[Ca^{2+}]_{o/i}$ was 39 kJ/mol in heart, 28 kJ/mol in liver under the conditions studied, and 23 kJ/mol in red cell (Table 3). The $\Delta G'[Ca^{2+}]_{o/i}$ in heart was approximately twice the $\Delta G'[Na^+]_{o/i}$ (Fig. 3), suggesting near equilibrium of the $2Na^+/Ca^{2+}$ exchanger, but in liver and red cell the $\Delta G'[Na^+]_{o/i}$ was only one third of that of $\Delta G'[Ca^{2+}]_{o/i}$, suggesting a $3Na^+/Ca^{2+}$ exchanger. Both stoichiometries have been reported. Intracellular $[Na^+]$, although subject to large errors in measurement, yielded a $\Delta G'[Na^+]_{o/i}$ of 17 kJ/mol in heart, decreasing to 10 kJ/mol in liver and 7 kJ/mol in red cell. The $\Delta G'[K^+]_{o/i}$ was 0 in heart but changed to -7 kJ/mol in liver and -8 kJ/mol in red cell, equivalent to the decrease in $\Delta G'[Na^+]_{o/i}$ (Fig. 3). The difference in energy between the plots of $\Delta G'[Na^+]_{o/i}$ and $\Delta G'[K^+]_{o/i}$ was 17 kJ/mol, which would be $3 \times 17 = 51$ kJ for the movement of $3Na^+$ versus K^+. This value approached the $\Delta G'$ of ATP hydrolysis, which varied between -54 and -58 kJ/mol, demonstrating that the $3Na^+/2K^+$ ATPase was close to equilibrium in all tissues studied.

The $\Delta G'[Mg^{2+}]_{o/i}$ was 15 kJ/mol in heart, but decreased to negligible values in red cell (Fig. 3). Although the stoichiometry of Mg^{2+} transport has yet to be determined, it is noteworthy that the $\Delta G'[H_2PO_4^-]_{o/i}$ was -15 kJ/mol in heart and approaching 0 in red cell, raising the possibility of a Mg^{2+}-$H_2PO_4^-$ cotransport

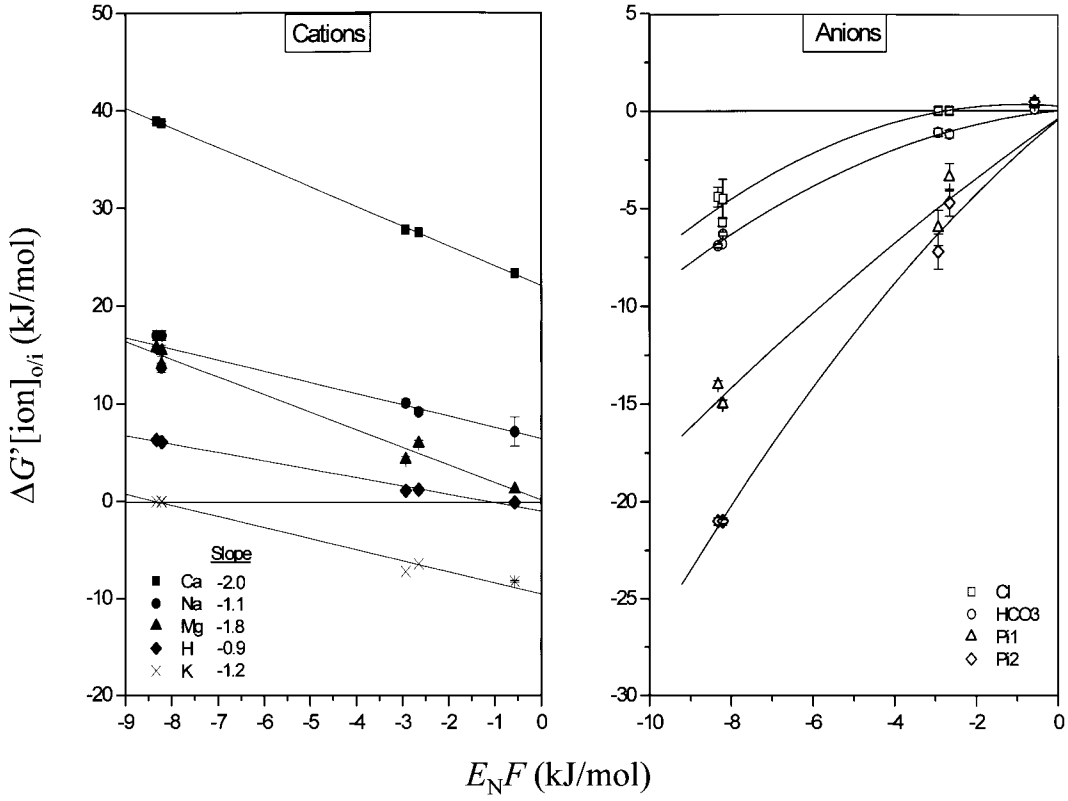

Figure 3. The ion transfer potentials of the nine major inorganic ions from intra- to extracellular phase of cells with differing electric potentials between phases. On the x-axis are plotted E_N times F. On the y-axis are plotted the mean $\Delta G'[ion^{\pm z}]_{o/i} \pm$ SEM for each of the ions (n given in Materials and Methods) calculated from $\Delta G'[ion^z]_{o/i} = RT \ln \frac{[ion^z]_o}{[ion^z]_i} - zFE_N$ (Eq. [2]). The $\Delta G'[ion^{\pm z}]_{o/i}$ represents the energy required to transfer 1 mole of the ion from the intra- to extracellular phase and is therefore a transfer potential analogous to a redox potential transferring an electron (*45*) or a group transfer potential (*46*) transferring a phosphate group. In heart, $\Delta G'[K^+]_{o/i}$ was 0, indicating it was in chemical and electrical equilibrium between the two phases. In contrast, $\Delta G'[Cl^-]_{o/i}$ was -4.5 to -5.7 kJ/mol, showing that Cl^- was actively pumped into the heart. In liver and red cell, the situation reversed. $\Delta G'[Cl^-]_{o/i}$ was 0 and $\Delta G'[K^+]_{o/i}$ was -6.4 to -7.2 kJ/mol in liver and -8.2 kJ/mol in red cell, indicating that K^+ was pumped into both red cell and liver. The slopes of the variation of $\Delta G'[Ca^{2+}]_{o/i}$ and $\Delta G'[Mg^{2+}]_{o/i}$ with $E_N F$ were -2 and -1.8, approximating their valence of $+2$. The slope of $\Delta G'[Na^+]_{o/i}$ was -1.1, $\Delta G'[K^+]_{o/i}$ was -1.2, and $\Delta G'[H^+]_{o/i}$ was -0.9, approaching 1. The $\Delta G'[ion^z]$ of all ions that were not zero, that is, K^+ in heart and Cl^- in liver and red cell were functionally Donnan active ions, the sum concentrations of which, plus the impermeant polyanions, ensure equality of H_2O activity on both sides of the plasma membrane, and thereby maintain constant cellular volume.

Table 3
Concentration of extra- and intracellular inorganic ions and $\Delta G'[\text{ion}^z]_{o/i}$ in heart, liver, and red cell

	Perfused heart									Liver						Red cell		
	Glucose (8)			G + Insulin (5)			G + Ketones (5)			Control (11)			+ Na acetate (6)			Control (7)		
Ion	EC	IC	$\Delta G'$	EC	IC	$\Delta G'$	EC	IC	$\Delta G'$	EC	IC	$\Delta G'$	EC	IC	$\Delta G'$	EC	IC	$\Delta G'$
Ca^{2+}	1.1	0.0002	38.7 ± 0.1	1.1	0.0002	38.9 ± 0.2	1.1	0.0002	38.7 ± 0.2	1.1	0.0002	27.5	1.07	0.0002	27.8	1.07	0.0002	23.4
Na^+	144	6.5 ± 5.2	13.7 ± 0.5	144	5.6 ± 1.8	17 ± 0.5	149	5.1 ± 0.8	17 ± 0.5	146 ± 1	12.3 ± 1.2	9.2 ± 0.3	170 ± 2	10.7 ± 1.5	10.1 ± 0.4	144	8.8 ± 6.3	7.18 ± 1.5
Mg^{2+}	0.5	1.2 ± 0.03	14 ± 0.02	0.5	0.72 ± 0.3	15.7 ± 0.2	0.5	0.74 ± 0.1	15.4 ± 0.6	0.52 ± 0.0	0.43 ± 0.0	5.97 ± 0.3	0.51 ± 0.02	0.97 ± 0.01	4.3 ± 0.3	0.52 ± 0.02	0.5	1.23
pH	7.42	7.06 ± 0.01	6.1 ± 0.03	7.39	7.05 ± 0.2	6.3 ± 0.05	7.4	7.04 ± 0.03	6.1 ± 0.07	7.37 ± 0.03	7.12 ± 0.07	1.21 ± 0.2	7.52 ± 0.0	7.12 ± 0.1	1.11 ± 0.2	7.40	7.29 ± 0.0	−0.1
K^+	5.9	142 ± 3	0	5.9	147 ± 5	0	5.9	141 ± 6	0	5.22 ± 0.1	175 ± 1	−6.4 ± 0.0	3.9 ± 0.3	229 ± 2	−7.2 ± 0.0	5.16 ± 0.3	153 ± 5	−8.2 ± 0.1
Cl^-	127	47.9 ± 3.6	−5.7 ± 0.2	127	29.4 ± 5.5	−4.4 ± 0.5	127	36.1 ± 11	−4.5 ± 1	103 ± 1	36.7 ± 2.3	0 ± 0.2	95.4 ± 1	30.8 ± 2.2	0 ± 0.2	108 ± 1	83.4 ± 2.9	0.1 ± 0.0
HCO_3^-	25	14.3 ± 0.2	−6.8 ± .0	25	14.4 ± 0.5	−6.9 ± 0.1	25	12 ± 0.4	−6.3 ± 0.1	26.7 ± 0.5	15.1 ± 1.1	−1.2 ± 0.2	36.5 ± 1.4	19.0 ± 1.6	−1.1 ± 0.2	26.7 ± 0.5	22 ± 0.7	0.1 ± 0.0
$H_2PO_4^-$	0.18	2.43 ± 0.2	−15 ± 0.2	0.19	1.8 ± 0.2	−14 ± 0.2	0.19	2.9 ± 0.2	−15 ± 0.2	0.22 ± 0.01	0.356 ± 0.08	−3.4 ± 0.7	0.11 ± 0.01	0.48 ± 0.01	−6.0 ± 0.9	0.39 ± 0.01	0.27 ± 0.02	0.36 ± 0.2
HPO_4^{2-}	0.91	5.4 ± 0.4	−21 ± 0.2	0.90	4.03 ± 0.3	−21 ± 0.2	0.91	6.26 ± 0.4	−21 ± 0.1	0.95 ± 0.03	0.91 ± 0.2	−4.7 ± 0.7	0.67 ± 0.04	1.55 ± 0.45	−7.2 ± 0.9	1.9 ± 0.1	1.0 ± 0.1	0.46 ± 0.2
ΔG_{ATP}			−54.2 ± 0.6			−58.0 ± 0.2			−57.0 ± 0.3			−56.5 ± 0.4			−56.1 ± 0.7			−57.1 ± 0.4
ΔG_{Ions}			53.3 ± 0.1			59.7 ± 2.5			59.0 ± 1.8			54.0 ± 0.7			60.3 ± 1.1			53.0 ± 1.7
Net			−0.9			1.7			2.0			−2.5			4.2			−4.1

The values are given as means ± SEM in units of μmol/ml intracellular H_2O, with number of determinations given in parentheses. For method of determination see text. Extracellular concentrations in perfusion fluid or plasma are given without SEM and were taken to be the same for all samples since they were analyzed on different samples than were intracellular measurements. The free intracellular $[Ca^{2+}]$ values were assigned as 0.2 μM in all tissues. Mg^{2+}, $H_2PO_4^-$, and HPO_4^{2-} are free concentration calculated as described in the text. The $\Delta G'$ ATP in kJ/mol is calculated from Eq. [8] and metabolite measurements as described in the text and corrected for the tissue free $[Mg^{2+}]$ and pH. $\Delta G'[\text{ion}^z]_{o/i}$ is given in kJ/mol from an empirical relationship defined in the text and is the sum of the $\Delta G'$ of each individual ion as given in:

$$RT \ln \frac{[Ca^{2+}]_o[Na^+]_o^2[Mg^{2+}]_i[H^+]_i[K^+]_i^2[Cl^-]_o[HCO_3^-]_i[H_2PO_4^-]_o[HPO_4^{2-}]_i}{[Ca^{2+}]_i[Na^+]_i^2[Mg^{2+}]_o[H^+]_o[K^+]_o^2[Cl^-]_i[HCO_3^-]_o[H_2PO_4^-]_i[HPO_4^{2-}]_o}$$

system. In perfused heart, the $\Delta G'[Na^+]_{o/i}$ was equal in magnitude and opposite in sign to the $\Delta G'[H_2PO_4^-]_{o/i}$, compatible with a near-equilibrium condition in the reaction catalyzed by the Na-Pi cotransporter (*31*)

$$Na_o^+ + H_2PO_{4o}^- \leftrightarrow Na_i^+ + H_2PO_{4i}^-$$

However in liver, the $\Delta G'[H_2PO_4^-]$ of -3 to -6 kJ/mol was significantly lower than the $\Delta G'[Na^+]_{o/i}$ of 9 to 10 kJ/mol, but approached the energy of $\Delta G'[Mg^{2+}]_{o/i}$, which ranged from 4 to 6 kJ/mol, suggesting that either Na-$H_2PO_4^-$ transport is out of equilibrium or that a different transport mechanism is involved, perhaps with Mg^{2+}. The $\Delta G'[H^+]_{o/i}$ ranged from 6.1 to 6.3 kJ/mol in perfused heart, or about one third of the $\Delta G'[Na^+]_{o/i}$, decreased to 1.1 to 1.2 kJ/mol in liver and to essentially 0 in red cell. Reflecting the permeance of CO_2 to cellular membranes, the $\Delta G'[HCO_3^-]_{o/i}$ was equal in magnitude and opposite in sign to $\Delta G'[H^+]_{o/i}$. In red cell, only the energy gradients of Ca^{2+}, Na^+, Mg^{2+}, and K^+ were greater than ± 1 kJ/mol, with the energy of all other ion gradients approaching zero.

The slopes of $\Delta G'[Na^+]_{o/i}$ and $\Delta G'[K^+]_{o/i}$ with $E_N F$ were -1.1 and -1.2, respectively (Fig. 3). The slopes of $\Delta G'[Ca^{2+}]_{o/i}$ and $\Delta G'[Mg^{2+}]_{o/i}$ were -2.0 and -1.8, respectively. The slope of $\Delta G'[H^+]_{o/i}$ was -0.85 whereas that of $\Delta G'[HCO_3^-]_{o/i}$ was 0.92. These values, with a change of sign, approximate the valence of the ion.

entirely by the energetics of the system, even though ion transport is catalyzed by a series of complex enzymatic reactions involving ATP-dependent pumps, exchangers, cotransporters, and ion channels. The plots of the changes in $\Delta G'[\text{anions}]_{o/i}$ intersected 0 kJ/mol at -6 mV, suggesting that the anionic distribution responded to the intracellular polyanionic metabolite excess. The intracellular negativity of the red cell was entirely due to the metabolite polyanions, with negligible contribution from permeant anion pumping.

The finding that $\Delta G'[Na^+]_{o/i}$ was 17 kJ/mol greater than that of $\Delta G'[K^+]_{o/i}$, approximating one third of the $\Delta G'_{ATP}$, indicated near equilibrium in the Na pump. The linear variation of all $\Delta G'[\text{cation}]_{o/i}$ with $E_N F$, having slopes conforming to their negative valences (Fig. 3), showed that the extent of the cationic gradients was determined solely by the E_N and the $\Delta G'_{ATP}$.

The linkage of the transport of inorganic ions to the E_N, the $\Delta G'_{ATP}$ and the $\Delta G'[Na^+]$ and its ancillary transport systems, such as the Na^+/Ca^{2+} exchanger, the Na^+-Pi cotransporter, the Cl^-/HCO_3^- exchanger, and other as yet undefined systems, resulted in a network of ion gradients energetically linked to one another in a coherent manner, representing the energy differences between the various inorganic ion gradients. We empirically derived a statement to relate the energy between phases of the major inorganic ions in an electroneutral, osmoneutral manner:

$$\Delta G'_{ATP} + RT \ln \frac{[Ca^{2+}]_o[Na^+]_o^2[Mg^{2+}]_i[H^+]_i[K^+]_i^2[Cl^-]_o[HCO_3^-]_i[H_2PO_4^-]_o[HPO_4^{2-}]_i}{[Ca^{2+}]_o[Na^+]_i^2[Mg^{2+}]_o[H^+]_o[K^+]_o^2[Cl^-]_i[HCO_3^-]_o[H_2PO_4^-]_i[HPO_4^{2-}]_o} \approx 0 \quad [8]$$

DISCUSSION

For the first time, to our knowledge, the energies of the major inorganic ion distributions have been calculated for three different tissues with widely differing E_N under six different physiological conditions. We found that all $\Delta G'[\text{cations}]_{o/i,}$ except K^+, had positive values (Fig. 3), showing active transport of cations out of the cells, where they formed functionally impermeant cationic excess Gibbs-Donnan active material. All $\Delta G'[\text{anions}]_{o/i}$, except Cl^- in liver and red cell, had negative values, showing active transport of anions into the cells, where they formed functionally impermeant anionic excess Gibbs-Donnan active material. The energies of the ion distributions were dependent on the $\Delta G'_{ATP}$ via the Na^+ pump and its linked transporters.

The observation that the slopes of the variation of $\Delta G'[\text{cation}]_{o/i}$ with $E_N F$ approximated their valence (Fig. 3) suggests that these slopes were transfer potentials representing the $\Delta G'$ per mole of charge transferred from the intra- to the extracellular phase. Such behavior would be expected in the transfer of ions between two electrodes in solution. This finding in living cells shows that the cationic gradients are determined

The value of the ionic term ranged from 53 to 60 kJ in heart, from 54 to 60 kJ in liver, and 53 kJ in red cell, whereas the $\Delta G'_{ATP}$ ranged from -54 to -58 kJ/mol (Table 3), making the net energy of ion movement approach zero or equilibrium. Because $[H^+]$ was over three orders of magnitude less than those of the other ions, it was considered to move with electrical, but not with osmotic effect. This empirically derived electroneutral and osmoneutral statement suggests a system of variable stoichiometries in tissues with differing ionic permeances and ionic gradients, the sum energy of which is determined by the $\Delta G'_{ATP}$.

The voltage of $E[K^+]_{o/i}$ of -80 to -90 mV in all tissues (Fig. 2) indicated that, during opening of a K^+ channel, either in an excitable tissue at rest or a nonexcitable tissue during hormonal stimulation, the E_N measured by intracellular electrode would approach -80 to -90 mV. However, during the opening of a Na^+ channel, the measured potential would approach equilibrium with the $E[Na^+]_{o/i}$ of 55 to 90 mV, as is observed during the transient action potential of excitable tissues such as nerve, muscle, and heart.

In a classical, inert Gibbs-Donnan equilibrium system containing impermeant polyanionic material in the inner phase

(Fig. 1), the ratio of the permeant monovalent ions, $[K^+]$ and $[Cl^-]$, between the phases would be the same, that is, they would assume the Donnan ratio, r_D, where:

$$r_D = \frac{[\text{cation}^+]_i}{[\text{cation}^+]_o} = \frac{[\text{anion}^-]_o}{[\text{anon}^-]_i}$$

because all permeant ions distribute according to the E_N between the phases. The essential feature of this in vitro Gibbs-Donnan system is that the distribution of all the permeant ions conforms to the Nernst electric potential between the phases and, as such, have $\Delta G'$ of zero because the electrical work and concentration work are equal in magnitude and opposite in sign (Eq. [2]). In cellular systems, the distribution of only one ion, K^+, in heart and Cl^- in liver and red cell conforms to the Nernst potential, thereby forming monoionic Gibbs-Donnan systems. The intracellular excess of permeant anions, coupled with excess extracellular permeant cations, equalizes the activity of the H_2O in the two phases and results in an increased electric potential between phases.

The origin of the resting electrical potential between the phases of a cell has been described by the Goldman field equation (*32*, *33*):

$$E_{rev} = \frac{RT}{F} \ln \frac{\rho_K[K]_o + \rho_{Na}[Na]_o + \rho_{Cl}[Cl]_i}{\rho_K[K]_i + \rho_{Na}[Na]_i + \rho_{Cl}[Cl]_o} \qquad [9]$$

where ρ is the relative permeability of ions, which in muscle has been taken to be $\rho[K]$: $\rho[Na]$: $\rho[Cl] = 1.0{:}0.04{:}0.45$ (*34*).

It has been argued that the Goldman equation represents a dissipative nonequilibrium steady state, essentially a K^+ diffusion potential. However, we show that $\Delta G'[K^+]_{o/i}$ is zero in heart (Table 3), therefore there can be no diffusion because the chemical energy is equal and opposite to the electrical energy of K^+. Although initially empirical (*35*), the Goldman equation was later justified as a derivative of the Plank-Einstein diffusion equation that requires that the flux $J_{Na\,in} = J_{K\,out}$ and that the movement of one ion cannot be altered by the movement of another (*33*). It is difficult to conceive how these fluxes can be equal if they are truly independent, as is required for the derivation of this formulation (*35*), particularly because the permeability of Cl^- is much greater than that of Na^+, requiring that $J_{Na\,in} + J_{K\,out} - J_{Cl\,in} = 0$.

In the same Goldman-based analysis, intracellular Cl^- was thought to reach electrochemical equilibrium with the potential set by the K^+ diffusion potential (*33*) and therefore not to contribute to the resting membrane potential despite its high permeance (*36*). However, in agreement with other studies (*37*, *38*), the data presented here show that in heart the $E[Cl^-]_{o/i}$ of -25 to -35 mV differs markedly from $E[K^+]_{o/i}$ of -85 to -86 mV (Fig. 3) and therefore was not set by the potential of the K^+ ion. Our values agree with previously reported values for heart $[Cl^-]_i$ in various species, which range from 20 to 37 mM (*37*, *38*).

It has also been argued that, because of the high permeance of Cl^- in heart, it is passively distributed with the membrane potential, which varies from about -90 mV at rest to 30 mV during an action potential, with the result that $E[Cl^-]_{o/i}$ reflects the average potential, not the resting potential (*39*). This inference was not confirmed by experimental data (*37*), which showed that $E[Cl^-]_{o/i}$ was less negative than $E[K^+]_{o/i}$ in beating and resting frog heart.

If the measured values for intra and extracellular ion concentrations (Table 3) are substituted into the Goldman equation (Eq. [9]) using the relative permeance factors listed previously, the calculated electrical potentials do not agree with those measured using intracellular KCl microelectrodes (Table 4). Only a

Table 4
Calculated and measured electrical potential between extra- and intracellular phases of cells

Tissue	Voltage calculated from the Goldman equation (mV)	Voltage calculated from the Nernst equation for the most permeant ion (mV)	Voltage measured with intracellular KCl electrodes (mV)
Heart	-48 to -57	-86	-83
Liver	-47 to -52	-27.5	-28

The voltages were calculated using the concentrations given in Table 1 and the Goldman equation (Eq. [9] in text):

$$E_{rev} = \frac{RT}{F} \ln \frac{\rho_K[K]_o + \rho_{Na}[Na]_o + \rho_{Cl}[Cl]_i}{\rho_K[K]_i + \rho_{Na}[Na]_i + \rho_{Cl}[Cl]_o}$$

where $\rho[K]$: $\rho[Na]$: $\rho[Cl] = 1.0$: 0.04: 0.45, or the Nernst equation (Eq. [1] in text):

$$E_{ion} = \frac{RT}{zF} \ln \frac{[\text{ion}^z]_o}{[\text{ion}^z]_i}$$

and the concentration of K^+ for heart or Cl^- for liver. The voltages measured with KCl microelectrodes are from the references (*28*, *15*).

value of 0 for ρ_{Na} and ρ_{Cl} in heart, or ρ_K and ρ_{Na} in liver and the setting of ρ_K in heart and ρ_{Cl} in liver to 1, give values in Eq. [9] that approximate those of the resting electric potential observed by intracellular KCl electrode measurements. By reducing these relative permeability factors to 0, and assigning the permeability factor of the most permeant ion to 1, the Goldman equation (Eq. [9]) is reduced to the standard Nernst equation (Eq. [1]).

Injury to a cell causes a decrease in $\Delta G'_{ATP}$ that leads to death via one of two major pathways; necrosis, which entails a stereotypic reaction wherein the cell loses K^+, gains Na^+ (*40*) and swells (*41*), and apoptosis (*42*), which results from activation of complex signaling pathways (*43*), causing changes in mitochondrial structure, extrusion of intracellular ions, and water with proteolysis. Both ultimately involve changes in mitochondrial energy generation. Until World War II, it was not recognized that the rise in serum K^+ associated with severe injuries could lead to death due to the depolarization of the heart, in which K^+ is the permeant ion. It is imperative that cellular energy in the form of $\Delta G'_{ATP}$ be considered a determining factor in the distribution of ions. The relationship between ion gradients and electric potential underscores the importance of maintaining cellular metabolic energy in the form $\Delta G'_{ATP}$, when maintaining or restoring ionic and water homeostasis after cellular injury.

The Goldman equation (Eq. [9]) has provided useful insights into the changing permeability of the ion channels responsible for the generation of the action potentials of excitable tissue. It seems less satisfactory as a description of the mechanisms responsible for the resting electrical potential between the extra- and intracellular phases of cells. Our data suggest that the resting electric potential is an inherent part of a Gibbs-Donnan equilibrium system created by excesses of functionally impermeant cations and anions dependent upon the energy of ATP-driven ion pumps and linked to each other through a series of exchangers and cotransporters sharing common ionic gradients.

ACKNOWLEDGEMENTS

The authors thank Carol Davey for her invaluable assistance with the manuscript and figures and the British Heart Foundation for their support.

REFERENCES

1. Nernst, W. (1888) Zur kinetik der in losung befindlichen korper: Theorie der diffusion. *Z. Phys. Chem.* **3**, 613–637.
2. Donnan, F. G. (1924) The theory of membrane equilibria. *Chem. Rev.* **1**, 73–90.
3. Gibbs, J. W. (1875) On the equilibrium of heterogeneous substances. *Trans. Conn. Acad. Arts Sci.* **3**, 108–248, 343–524.
4. Van't Hoff, J. H. (1885) L'Equilibre chimique dans les systems gazeuz ou dis a l'etal dilue. *Arch. Neerl.* **20**, 239–302.
5. Leaf, A. (1956) On the mechanism of fluid exchange in tissue in vitro. *Biochem. J.* **62**, 241–248.
6. Peterson, G. L., Churchill, L., Fisher, L. E., and Hokin, L. E. (1982) Structure and biosynthesis of (Na,K)-ATPase in developing brine shrimp nauplii. *Ann. N. Y. Acad. Sci.* **402**, 185–206.
7. Bernard, C. (1878) *Lecons sur les Phenomenes de le Vie Communs aux Animaux et aux Vegetaux*. J. B. Bailliére, Paris.
8. Skou, J. C. (1964) Enzymatic aspects of active linked transport of Na^+ and K^+ through cell membranes. *Prog. Biophys. Mol. Biol.* **14**, 133–166.
9. Tanford, C. (1981) Equilibrium state of ATP-driven pumps in relation to physiological ion concentration gradients. *J. Gen. Physiol.* **77**, 223–229.
10. Masuda, T., Dobson, G. P., and Veech, R. L. (1990) The Gibbs-Donnan near-equilibrium system of heart. *J. Biol. Chem.* **265**, 20321–20334.
11. Veech, R. L., Gitomer, W. L., King, M. T., Balaban, R. S., Costa, J. L., and Eanes, E. D. (1986) The effect of short chain fatty acid administration on hepatic glucose, phosphate, magnesium and calcium metabolism. *Adv. Exp. Med. Biol.* **194**, 617–646.
12. Sato, K., Kashiwaya, Y., Keon, C. A., Tsuchiya, N., King, M. T., Radda, G. K., Chance, B., Clarke, K., and Veech, R. L. (1995) Insulin, ketone bodies, and mitochondrial energy transduction. *FASEB J.* **9**, 651–658.
13. Huang, M. T., and Veech, R. L. (1988) Role of the direct and indirect pathways for glycogen synthesis in rat liver in the postprandial state. *J. Clin. Invest.* **81**, 872–878.
14. Kwack, H., and Veech, R. L. (1992) Citrate: its relation to free magnesium ion concentration and cellular energy. In *From Metabolite, to Metabolism to Metabolon* (Stadtman, E. R., and Chock, P. B., eds.). pp. 185–207, Academic Press, San Diego.
15. Veech, R. L., Gates, D. N., Crutchfield, C. W., Gitomer, W. L., Kashiwaya, Y., King, M. T., and Wondergem, R. (1994) Metabolic hyperpolarization of liver by ethanol: the importance of Mg^{2+} and H^+ in determining impermeant intracellular anionic charge and energy of metabolic reactions. *Alcohol Clin. Exp. Res.* **18**, 1040–1056.
16. Walser, M. (1967) Magnesium metabolism. *Ergeb. Physiol.* **59**, 185–296.
17. Veloso, D., Guynn, R. W., Oskarsson, M., and Veech, R. L. (1973) The concentrations of free and bound magnesium in rat tissues. Relative constancy of free Mg^{2+} concentrations. *J. Biol. Chem.* **248**, 4811–4819.
18. Sillen, L. G., and Martell, A. E. (1964) *Stability Constants of Metal Ion Complexes*. Burlington House, London.
19. Walser, M. (1971) Symposium International sur le Deficit Magnesium in Pathologic Humaine. In *Symposium International sur le Deficit Magnesium in Pathologic Humaine* (Durlach, J., ed.). pp. 55–63, SGEVM, Vittel.
20. Funder, J., and Wieth, J. O. (1966) Chloride and hydrogen ion distribution between human red cell and plasma. *Acta Physiol. Scand.* **68**, 234–245.
21. Dobson, G. P., Veech, R. L., Hoeger, U., and Passonneau, J. V. (1991) Enzymatic determination of total CO_2 in freeze-clamped animal tissues and plasma. *Anal. Biochem.* **195**, 232–237.
22. Clarke, K., Kashiwaya, Y., King, M. T., Gates, D., Keon, C. A., Cross, H. R., Radda, G. K., and Veech, R. L. (1996) The β/α peak height ratio of ATP: a measure of free $[Mg^{2+}]$ using ^{31}P NMR. *J. Biol. Chem.* **271**, 21142–21150.
23. Kashiwaya, Y., Sato, K., Tsuchiya, N., Thomas, S., Fell, D. A., Veech, R. L., and Passonneau, J. V. (1994) Control of glucose utilization in working perfused rat heart. *J. Biol. Chem.* **269**, 25502–25514.
24. King, M. T., Gamble, J. L. Jr., and Veech, R. L. (1979) Bicarbonate measurements in rat liver, brain, heart, and skeletal muscle. *Anal. Biochem.* **95**, 183–187.
25. Henderson, L. J. (1928) In *Blood, A Study of General Physiology, Silliman Lectures*. Yale University Press, New Haven.
26. Kim, Y. A., King, M. T., Teague, W. E., Jr., Rufo, G. A., Jr., Veech, R. L., and Passonneau, J. V. (1992) Regulation of the purine salvage pathway in rat liver. *Am. J. Physiol.* **262**, E344–E352.
27. King, M. T., Passonneau, J. V., and Veech, R. L. (1990) Radiometric measurement of phosphoribosylpyrophosphate and ribose 5-phosphate by enzymatic procedures. *Anal. Biochem.* **187**, 179–186.
28. Kleber, A. G. (1983) Resting membrane potential, extracellular potassium activity, and intracellular sodium activity during acute global ischemia in isolated perfused guinea pig hearts. *Circ. Res.* **52**, 442–450.
29. Veech, R. L., Lawson, J. W. R., Cornell, N. W., and Krebs, H. A. (1979) Cytosolic phosphorylation potential. *J. Biol. Chem.* **254**, 6538–6547.

30. Ohm, G. S. (1827) *Die galvanische Kette: mathematisch bearbeitet*. T. H. Reimann, Berlin.
31. Peterson, G. L., Churchill, L., Fisher, L. E., and Hokin, L. E. (1982) Structure and biosynthesis of (Na,K)-ATPase in developing brine shrimp nauplii. *Ann. N.Y. Acad. Sci*. **402**, 185–206.
32. Rana, A., Sathyanarayana, P., and Lieberthal, W. (2001) Role of apoptosis of renal tubular cells in acute renal failure: Therapeutic implications. *Apoptosis*. **6**, 83–102.
33. Sato, K., Kashiwaya, Y., Keon, C. A., Tsuchiya, N., King, M. T., Radda, G. K., Chance, B., Clarke, K., and Veech, R. L. (1995) Insulin, ketone bodies, and mitochondrial energy transduction. *FASEB J*. **9**, 651–658.
34. Sillen, L. G., and Martell, A. E. (1964) *Stability constants of metal ion complexes*. London, Burlington House.
35. Sperelakis, N. (1979) Origin of the cardiac resting potential. In *Handbook of Physiology: the cardiovascular system* (Berne, R. M., Sperelakis, N., and Gieger, S. R., eds.). pp. 187–267. Am. Physiol. Soc., Bethesda.
36. Tabor, H., and Rosenthal, S. M. (1945) Effects of potassium administration, of sodium loss, and fluid loss in tourniquet shock. *Public Health Rep*. **60**, 401–419.
37. Van't Hoff, J. H. (1887) Die roll des Osmotischen druckes in der analogie zwischen losungen und gasen. *Z. Phys. Chem*. **1**, 481–508.
38. Veech, R. L., Gates, D. N., Crutchfield, C. W., Gitomer, W. L., Kashiwaya, Y., King, M. T., and Wondergem, R. (1994) Metabolic hyperpolarization of liver by ethanol: The importance of Mg^{2+} and H^{+} in determining impermeant intracellular anionic charge and energy of metabolic reactions. *Alcohol. Clin. Exp. Res*. **18**, 1040–1056.
39. Veech, R. L., Gitomer, W. L., King, M. T., Balaban, R. S., Costa, J. L., and Eanes, E. D. (1986) The effect of short chain fatty acid administration on hepatic glucose, phosphate, magnesium and calcium metabolism. *Adv. Exp. Med. Biol*. **194**, 617–646.
40. Veech, R. L., Kashiwaya, Y., and King, M. T. (1995) The resting potential of cells are measures of electrical work not of ionic currents. *Int. Physiol. Behav. Sci*. **30**, 283–306.
41. Veech, R. L., Lawson, J. W. R., Cornell, N. W., and Krebs, H. A. (1979) Cytosolic phosphorylation potential. *J. Biol. Chem*. **254**, 6538–6547.
42. Veloso, D., Guynn, R. W., Oskarsson, M., and Veech, R. L. (1973) The concentrations of free and bound magnesium in rat tissues. Relative constancy of free Mg^{2+} concentrations. *J. Biol. Chem*. **248**, 4811–4819.
43. Walser, M. (1971) Symposium International sur le Deficit Magnesium in Pathologic Humaine. In *Symposium International sur le Deficit Magnesium in Pathologic Humaine* (Durlach, J., ed.). pp. 55–63, Vittel, SGEVM.
44. Wehrle, J. P., and Pedersen, P. L. (1989) Phosphate transport processes in eukaryotic cells. *J. Membr. Biol*. **111**, 199–213.